

PAPER • OPEN ACCESS

Impact of wind turbine operation conditions on infrasonic and low frequency sound induced by on-shore wind turbines

To cite this article: Esther Blumendeller *et al* 2022 *J. Phys.: Conf. Ser.* **2265** 032048

View the [article online](#) for updates and enhancements.

You may also like

- [Prospects for generating electricity by large onshore and offshore wind farms](#)
Patrick J H Volker, Andrea N Hahmann, Jake Badger et al.
- [In situ observations of the influence of a large onshore wind farm on near-surface temperature, turbulence intensity and wind speed profiles](#)
Craig M Smith, R J Barthelmie and S C Pryor
- [Experimental study of the impact of large-scale wind farms on land-atmosphere exchanges](#)
Wei Zhang, Corey D Markfort and Fernando Porté-Agel



The Electrochemical Society
Advancing solid state & electrochemical science & technology

243rd ECS Meeting with SOFC-XVIII

More than 50 symposia are available!

Present your research and accelerate science

Boston, MA • May 28 – June 2, 2023

[Learn more and submit!](#)

Impact of wind turbine operation conditions on infrasonic and low frequency sound induced by on-shore wind turbines

Esther Blumendeller, Martin Hofsäß, Arne Goerlitz and Po Wen Cheng

Stuttgart Wind Energy at University of Stuttgart, Allmandring 5B, 70569 Stuttgart, Germany.

E-mail: blumendeller@ifb.uni-stuttgart.de

Abstract. In this paper, the influence of wind turbine operation conditions, like rotational speed, nacelle position and output power, on the low- and infrasonic sound emissions at the wind farm and sound immissions at residential buildings will be investigated. For this purpose, parallel measurements were carried out at a wind farm on the Swabian Alb in complex terrain and at four residential locations in the vicinity of the wind farm over a period of two months. Distinctive tones can be assigned to the blade passage at different rotational speeds. Furthermore, tones at 28.9 Hz (rated) and 18.3 Hz (below rated) with two higher harmonics can be attributed to the wind turbine generator. Wind farm infrasonic tones at the blade passing frequency were detected at the wind farm and residential buildings. At the residential buildings infrasonic tones were detected mainly for maximum rotational speed of the wind turbines and seem to be independent from wind direction.

1. Introduction

During operation, wind turbines (WTs) act as sound sources. There are two different mechanisms of sound generation from WT, which are of mechanical and aerodynamic origin. Mechanical noise can be generated by components such as the gearbox, the generator, the azimuth drives or the cooling fans. Since these are mostly rotating noise sources, the emissions usually have a tonal character [1, 2]. A reduction in noise emissions can be achieved here, for example, by using damping materials on the relevant component.

Aerodynamic noise is generated by the rotation of the rotor blades and thus the airflow around the blades. There are several mechanisms for sound generation like inflow turbulent noise caused by the interaction between incident vortices and the rotor blade surface [3, 4, 5]. Van Den Berg [6] divided the frequency spectrum in three ranges and noise generation mechanisms: Thickness sound, inflow turbulent sound and trailing edge sound. According to [6] the slowed wind caused by the tower leads to a velocity deficit and a change in the angle of attack as the rotor blade passes the tower, leading to thickness noise at the blade passing frequency. According to [7, 8], this mechanism is called loading noise, whereas thickness noise is mainly emitted in the rotor plane due to the displacement of surrounding air by the rotating blade. Besides different naming, it is undisputed that a change in angle of attack will result in sound emission. A cyclic variation will result in low frequency (20-200 Hz) and infrasonic (1-20 Hz) sound. However, thickness noise is only one possible mechanism for generating WT infrasound. Inflow turbulent



sound has broadband character in the low frequency range and trailing edge sound in the mid- and high frequency range is caused by air flowing over the blades.

Annoyance of residents in the vicinity of wind farms might be related to WT noise with infrasonic and low frequency noise content [9, 10]. Although infrasound from WTs is well below the human hearing threshold, it is not yet clear how it can contribute to the annoyance of residents [5]. Due to the long wavelength of low frequency and infrasound, the absorption of air is negligible and shielding by obstacles between the sound source and the receiver also has little effect [2]. The same applies to building facades, which are much smaller compared to the wavelength in the infrasound range. A relation to annoyance can be found if an indoor effect can be detected due to coupling of the infrasound with the building structure [11] or through resonances excited in the room by low frequency sound, which can even lead to higher sound pressure levels (SPL) indoors compared to outdoors [5]. In addition, the two mechanisms of air absorption and transmission loss of facades reduce the mid frequency components, which can lead to more pronounced low frequency components [5, 12]. In many studies, fluctuating SPL over time have also been associated with the blade passage, which modulates the broadband aerodynamic rotor blade noise at frequencies between 0.5 and 2 Hz [2, 6, 13].

Reducing mid frequency sound by control methods such as trailing edge serrations affecting acoustic scattering at the trailing edge, is relatively easy to implement and can still be adjusted on an erected WT. Control methods for the low and infrasonic frequency range are not as easy to implement [14]. Doolan [14] proposed an increased distance between rotor blade tip and tower to reduce the blade tower interaction or minor adjustments, for example to the rotor blade pitch. However, in order to effectively implement such measures, that lead to sound reduction at the point of immission, the mechanisms of low frequency and infrasound creation and atmospheric propagation need to be better understood. This requires a better understanding of the effects of meteorological conditions and WT operation, which can quickly vary with time, but also topography on the generation, propagation and perception of low frequency and infrasound.

The aim of this work is to investigate the influence of WT operation on the generation and propagation of low- and infrasonic sound and their acoustic characteristics based on measurement data.

2. Methodology

2.1. Measuring Location, Setup, and Periods

Acoustic measurements were conducted in the vicinity of a wind farm (WF) located on the Swabian Alb in southern Germany. The site is equipped with three GE 2.7 MW WTs (hub height 139 m, rotor diameter 120 m, 2.78 MW rated power) and close to an escarpment in 1 km distance to the municipality of Kuchen in a valley location. The difference in height between groundlevel of WT 3 and Kuchen is about 290 m. Acoustic measurements were carried out for approximately 54 days from 2020-10-22 to 2020-12-16.

Figure 1 shows a map of the WF and the measurement locations. WT 1 is surrounded by open field, while the other two WTs 2 and 3 are positioned in a forest. One microphone was placed 140 m south of WT 1 on a sound reflecting wooden plate with two hemispherical windshields to reduce the wind induced noise. At the residential buildings in approximately 1 km to 1.2 km distance to WT 3, referred to as measurement location at R1, R2, R3 and R4 (Figure 1), two more microphones were positioned outside and inside the building. The instrumentation at the point of immission was moved between residential locations every two weeks within the measurement period. While the outside microphone had the same set up as the WF microphone, the inside microphone was placed on a tripod in a dedicated room, which was the sleeping room at three residential buildings and a guest room at one measurement location. It should be noted that the window of the room at R2 was open during the entire measurement period, which resulted in a higher indoor SPL. All microphones measured the continuous time series of sound pressure

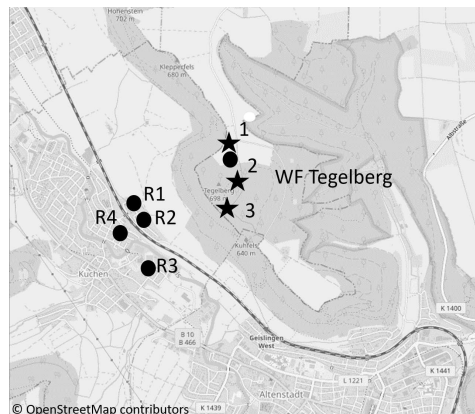


Figure 1: Map [15] with the locations of the wind turbines of wind farm Tegelberg (stars), and measurement locations at the wind farm and four residential buildings in Kuchen (circle). Acoustic measurement instruments were located at wind turbine 1.

with a sampling frequency of 20 kHz. For the outdoor measurements two G.R.A.S. 47AC 1/2 inch free-field condenser microphone sets were used. Indoor measurements were conducted with a Brüel&Kjaer 4964 1/2 inch free-field infrasound microphone with G.R.A.S. 26Cl preamplifier. All data were recorded with an imc CRONOSflex Audio2-4 system. Additionally meteorological measurements of wind speed and direction (with a 23 Hz sampling frequency), humidity, temperature and pressure (with a 10 Hz sampling frequency) were conducted at the WF site with a 10 m high met mast. More detailed information concerning the instrumentation, measurements, locations with surrounding conditions and schematics of the indoor measurement set-up can be found in [16, 17].

A cooperation with the turbine operator enabled regular nightly WT shutdowns of 20 min periods. In addition, the 10 min average WT operation data at hub height for all WTs was provided for the measurement period. During the measurement period the wind direction west-north-west occurred most frequently, with unusual contributions from the southeast direction as well [17]. In the present work, all timestamps are based on Coordinated Universal Time (UTC).

2.2. Data evaluation

By displaying the acoustic data in form of a spectrogram, a first impression over the data of several hours at all measuring locations is possible. The power spectral density (PSD with matplotlib [18]) of the acoustic data calculated with the following properties: time length $T=10$ s, rectangular window with length $N_{win} = T \cdot f_s$ for $f_s=500$ Hz, no averaging and 0 % overlap for a frequency range of 0.1-200 Hz and 0.1-30 Hz.

To obtain detailed information on the spectral content of the WT signature, a narrowband analysis is carried out. Narrowband spectra (spectrograms with scipy [19]) were calculated over 10 minute time periods for a time length $T=10$ s, Hanning window and window length $N_{win} = T \cdot f_s$ for $f_s=20$ kHz and 50 % overlap.

By using 10 min mean values of WT operating data and wind speed data at 10 m height, acoustic data were selected based on five criteria to evaluate the impact of WT operation on the acoustic character of the WT sound. These are defined ranges of rotational speed, nacelle position (is considered as wind direction at hub height in the following), wind speed at 10 m height, time of day and measurement period to consider frequency spectra separately for the different residential locations. The rotational speed of all WTs at the WF was defined as 11-

12.5 rpm for rated operation condition and 7.5-8.5 rpm for below rated operation condition. To determine the background noise, data of the periods with maximum rotational speed of 1 rpm of all WTs were selected. The wind direction at hub height is limited to 180-315° which corresponds to south and southwestern wind direction and upwind condition for the residential buildings. Wind speed at 10 m height was limited to 2 m/s, to reduce wind induced noise at the microphone. Only nighttime data from 00:00 to 05:00 UTC were considered to increase the contrast between ambient noise and WT sound data.

To avoid disturbance of the data by installation and calibration, data from days when the devices were set up are excluded. A correction for the reflection caused by mounting the two outdoor microphones on a wooden ground plate has not been done.

In previous investigations, the BPF and its harmonics in the infrasonic frequency range could be clearly assigned to the WT operation [16]. Following the publication by Zajamšek et al [20], the 4th harmonic of the BPF is detected to identify infrasound occurrences. A frequency range for the peak detection was defined for the rotational speeds from 10-12.5 rpm, thus the BPF of the WT is 0.5-0.625 Hz and the 4th harmonic considered in the range of 2-2.5 Hz. Additionally, this is the frequency range that has already been classified by [14] as the one with the energy maximum in the blade-tower interaction (BTI) noise. An algorithm calculates the narrowband spectrum over 10 min periods with the same properties mentioned beforehand. For peaks with a prominence of 6 dB above the background floor, the SPL and the respective frequency were captured. In Zajamšek et al [20], a value of 20 dB above background level was chosen. These values were not measured in this investigation. Spot checks of narrowband spectra of periods with detected peaks showed a clear presence of infrasound. The procedure can be based on the IEC 61400-11:2012 standard [21], where the maximum of a tone must exceed the average level of the masking sound by more than 6 dB.

3. Results

3.1. Power spectral density

To obtain an overview of the acoustic measurement data for all three locations (WF, outside, inside), spectrograms were calculated for the period of one exemplary day.

Figure 2a shows the operating data from 2020-10-26. It can be seen that WT 3 was shut down between 00:20 and 01:30 UTC, as well as WT 1 and WT 2, which are not shown here. Wind came mainly from west indicating that the residential building R1 is located in upwind direction, and the wind speed at hub height varied between 2 m/s and 10 m/s.

The shutdown time of the WTs is clearly visible in the acoustic data of the WF location on the basis of reduced PSD over the entire frequency range of about 1-200 Hz (see Figure 2b). Of particular interest are the signal components that are present only during WT operation. Below 10 Hz and varying in frequency range between 15 Hz and 120 Hz, several tones of increased density are observed that disappear immediately when the WT rotational speed drops to zero. The frequencies below 10 Hz appear to be directly correlated to the rotational speed of the WT as multiples of the BPF. Higher wind speeds in the morning hours lead to a higher spectral density intensity in the acoustic data at the WF in the considered frequency range.

The acoustic signals measured at the place of immission are shown in the middle and bottom PSD diagram. Here the shutdown of the WT is also recognizable on the basis of a reduced PSD diagram. In contrast to the higher multiples between 20 Hz and 80 Hz (Figure 2b), the multiples of the BPF and the 20 Hz fluctuating tone are still visible at the residential locations (Figure 2c). The signal component fluctuating with rotational speed between 80 Hz and 120 Hz is only faintly visible in the outdoor and indoor signals. The influence of higher wind speed leads to a slightly increased intensity, in both, the inside and outside location.

Furthermore, signal components related to the measurement location and other sound sources can be identified. The increased intensity at 13 Hz can be attributed to a resonance of the

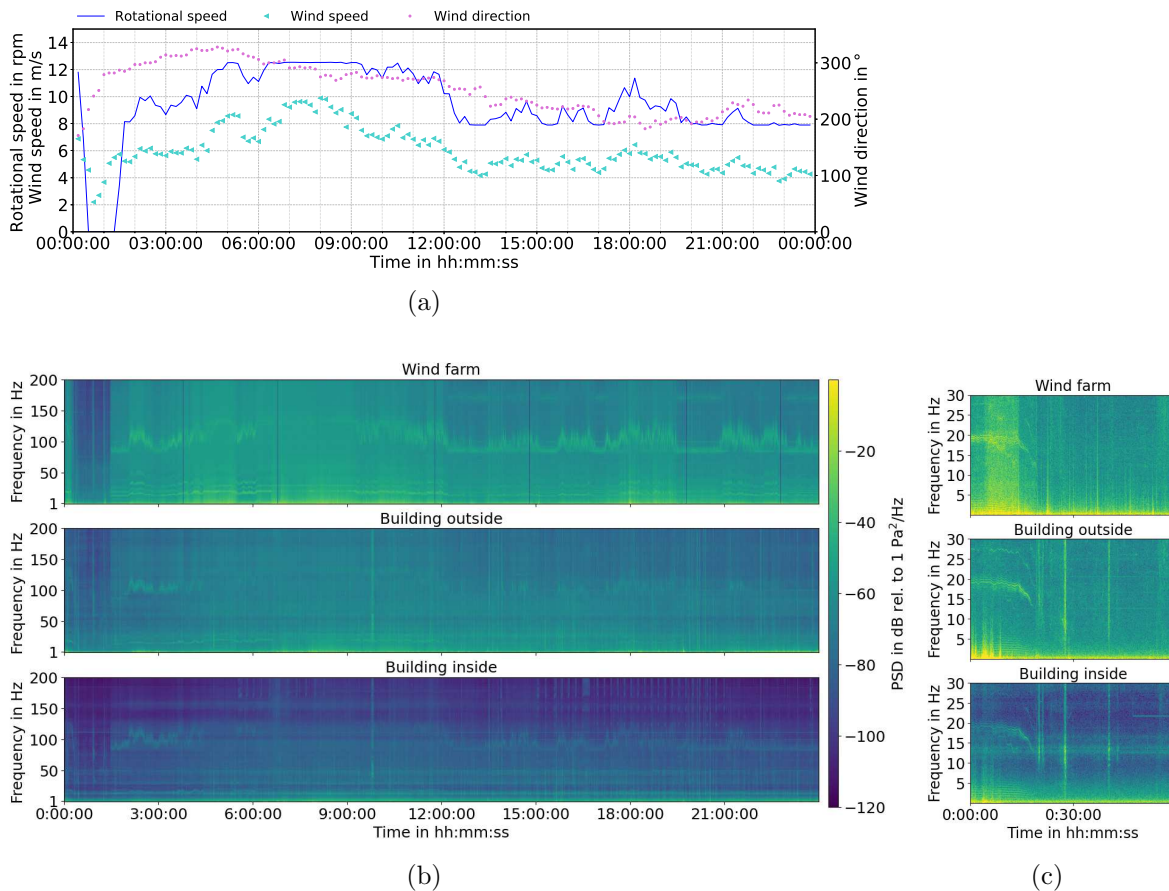


Figure 2: (a) Rotational speed, wind speed and wind direction in hub height of wind turbine 3. Power spectral density for a frequency range of 1-200 Hz (b) and 1-30 Hz (c) of all three measurement locations at the wind farm (top), outside (middle) and inside (bottom) of residential location R1.

building structure [9], constant tones at 50 Hz and 100 Hz to electrical noise. The vertical lines with high intensity both outside and inside can be caused by short duration sound sources like passing trains at 40 m distance.

3.2. Narrow band spectra

To determine the influence of the rotational speed on low frequency and infrasonic sound induced by WTs, the narrowband spectra are calculated for 10 min sections for the frequency range 0.1-200 Hz. The spectra are filtered based on the filter criteria mentioned in chapter 2.2 and averaged afterwards. Thus, the frequency spectra of the four measurement periods with rated and below rated WT operation can be compared with the background noise from shutdown periods. Data set sizes for rated/below rated/shutdown conditions were 23/27/27 for R1, 13/52/40 for R2, 21/11/1 for R3 and 12/16/15 for R4. Figures 3a-d show the narrowband spectra for the four measurement periods at resident R1 to R4.

The main difference between on/off spectra are tones below 10 Hz, around 20 Hz, 80 Hz and 120 Hz. Table 1 lists frequencies that occur in the narrow band spectra of the four measurement periods and can be attributed to WT operation since they cannot be identified in the background noise. Peaks below 10 Hz can be clearly assigned to the blade passage and higher harmonics. The BPF for rated operation is between 0.6 Hz and 0.625 Hz, and around 0.4 Hz for the below

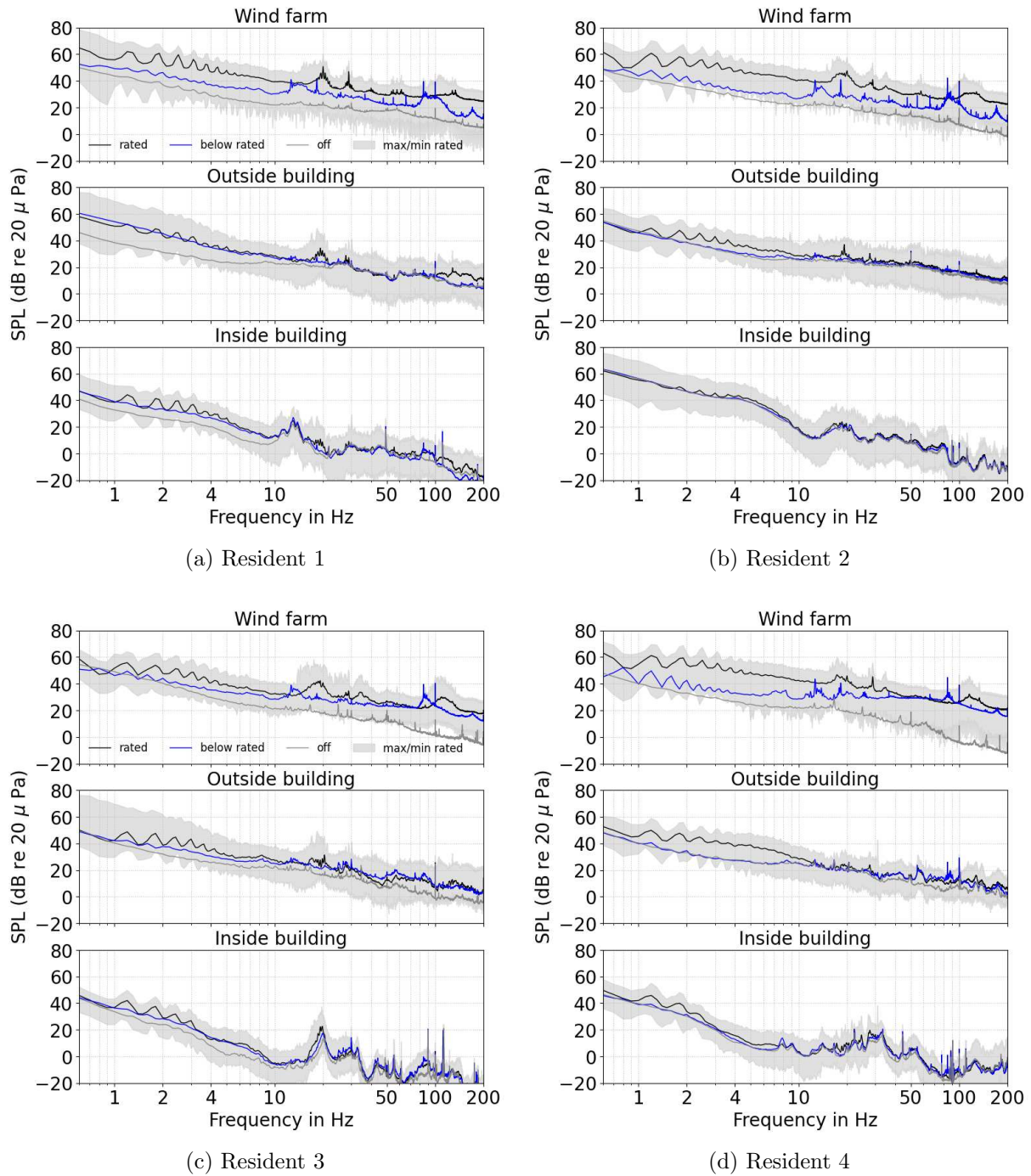


Figure 3: Comparison of mean narrowband spectra for the microphone position at the wind farm and residential building. Only night time data from 00:00-05:00 UTC for shut down (0-1 rpm), under rated (7.5-8.5 rpm) and rated (11-12.5 rpm) operation of wind turbine 3 is considered.

Table 1: Frequencies of tones attributed to WT operation divided into rated (11-12.5 rpm) and below rated (7.5-8.5 rpm) rotational speed conditions with origin of the tone.

WT operation	Frequency in Hz								Origin
	2.	3.	4.	5.	6.	7.	8.		
Harmonic of BPF	2.	3.	4.	5.	6.	7.	8.		
rated	1.2	1.89	2.5	3.0	3.69	4.4	5.0	Blade	
below rated	–	1.2	1.6	2.0	2.4	2.8	–	passing	
rated	28.9	57.8	86.8					Generator	
below rated	18.3	36.5	54.7						
rated	19.2	19.9	128.1						
below rated	12.5/12.6	–	84.4						

rated range. Therefore, the BPF for both operating conditions varies over frequency, which can be seen in particular by comparing the spectra of the WF location in Figure 3a-d. Furthermore the BPF and its harmonics is much more pronounced at rated conditions and not visible outside and inside the buildings for below rated conditions. Table 1 shows the 2nd to 8th harmonic of the BPF of up to 5 Hz for both operating conditions.

By considering the generator rotational speed for rated and below rated operation (with maximum 1746 rpm), both frequencies at 28.9 Hz and 18.3 Hz can be attributed to the generator. These tones are measured both at the WF and at all residents inside and outside the building. The 2nd and 3rd harmonic at 57.8 Hz/36.5 Hz and 86.7 Hz/54.7 Hz for rated/below rated rotational speed are measured at the WF location, but only partially at the residential buildings. All other peaks are related to the rotational speed, but the origin cannot be clearly identified. One conjecture is the connection with the gearbox of the WT, since the occurrence is strongly correlated with the rotational speed. In [22] a tone in the frequency range of 124 Hz with occasional shifts to 120 Hz, 126 Hz or 128 Hz within a WF with 2 MW WT was attributed to the gearbox, which is comparable to the 128 Hz tone during rated rotational speed.

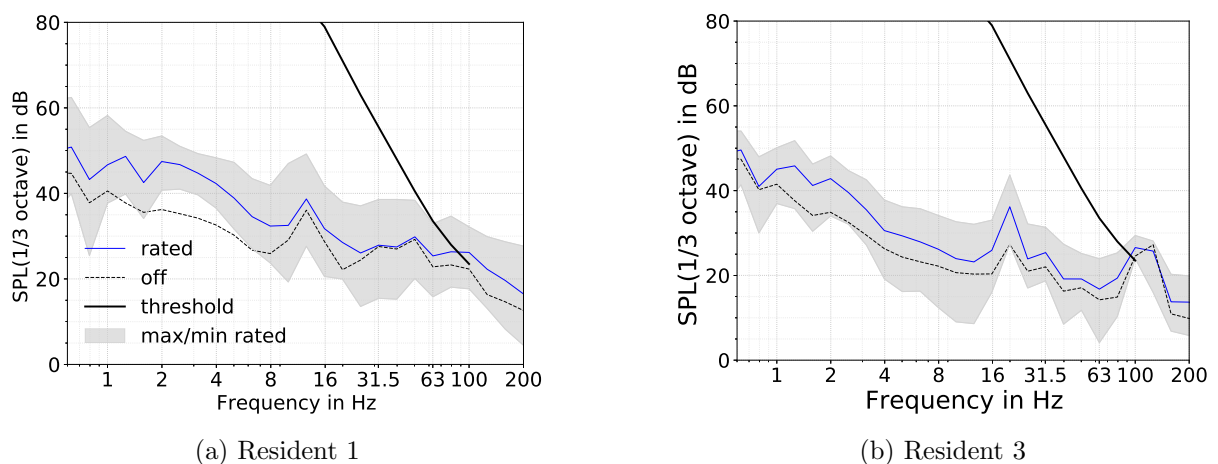


Figure 4: 1/3 octave spectra for the microphone position at the residential building R1 and R3. Only night time data from 00:00-05:00 UTC for shut down (0-1 rpm) and rated (11-12.5 rpm) operation of wind turbine 3 is considered.

By comparing background noise spectra with spectra during WT operation, tones can be

identified that are not attributable to WT operation. In the building broadband tones occur between 10 Hz and 20 Hz, which remain identical in all operating conditions and can be assigned to structural resonances at 13 Hz (R1), around 19 Hz (R2), 19.2 Hz (R3), 7.8 Hz, 9 Hz and 14 Hz (R4) due to [23, 24]. Furthermore sharp peaks at 50 Hz and 100 Hz can be attributed to electrical noise. Peaks at 90 Hz and 112 Hz, that occur only in the interior of all residents can be assigned to an acoustic sound caused by the measurement system.

However, the comparison of the SPLs with the human hearing threshold according to [25, 26] requires the calculation of a 1/3 octave spectrum. In order to be able to classify the levels measured in the building with regard to their audibility, the 1/3 octave spectrum for the same filter conditions and for rated operation during the measurement period of R1 and R3 (comparable to Figure 3a-b) is shown in Figure 4. As expected, the infrasonic tones are below the hearing threshold and is exceeded by maximum values at 63 Hz in Figure 4a. Similar values are also calculated for the measuring locations R2 to R4.

3.3. Infrasonic sound

In order to identify infrasonic occurrences, the SPL and frequency of the 4th blade pass harmonic was captured. Figure 5 shows occurrences of infrasound over the whole course of the measurement campaign for all microphone positions. At the WF location infrasound was captured most often, whereas occurrences lessen from outside to inside of the residential locations, just as the SPL decreases over this distance. There is no data available from the measurements at the residential building between 2020-10-29 and 2020-11-12 due to failed data storage, which is the reason for only infrasound occurrences at the WF location.

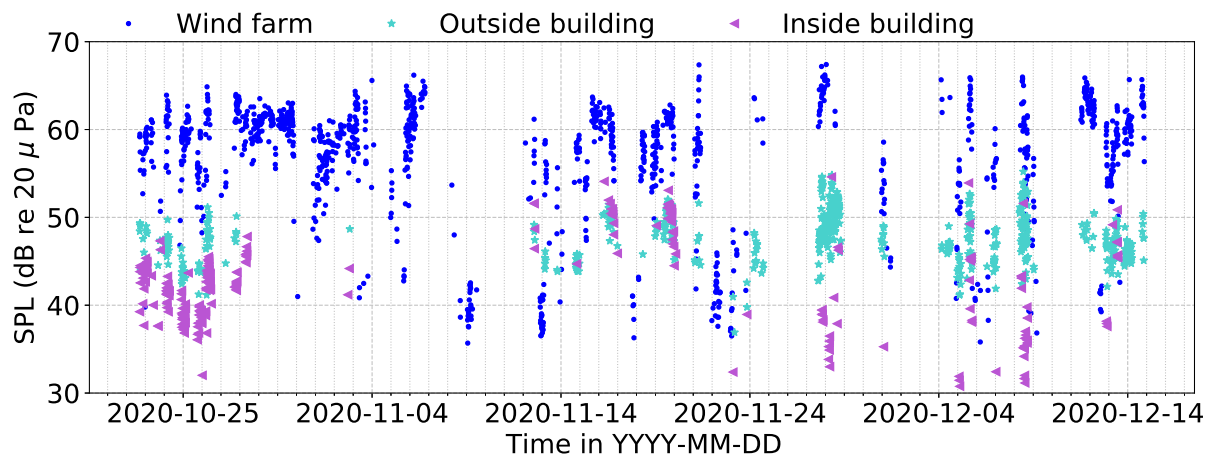


Figure 5: Sound pressure level of 4th blade passing frequency harmonic for the measurement period October to December 2020 at all measurement locations (wind farm and residential buildings).

Due to the defined frequency range for the 4th BPF, a range of rotational speeds was detected. From Figure 6 it can be seen, that infrasound at the WF location was detected for all considered rotational speeds from 10-12.5 rpm (indicated by the frequency of the 4th harmonic 2-2.5 Hz). Highest SPL are related to rated rotational condition. Looking at the residential locations, infrasound is mainly detected for rated condition with rotational speeds between 12 rpm and 12.5 rpm. The scattering of SPL indoors can be explained by the different conditions in the buildings. For example, the open window at resident 2 resulted in higher 4th harmonic levels of about 50 dB, while the levels at R1, R3, and R4 were about 35-50 dB.

The relation of infrasound occurrence with rotational speed and wind speed at hub height of WT 3 is shown in Figure 7a. It clarifies the relation between increasing SPL of the infrasonic peak with increasing rotational rate with almost constant SPL above a wind speed of 7 m/s. Since the WF microphone is positioned at WT 1, but the infrasound occurrences are related to the data of WT 3 (which is closest to the residential locations), it can happen that infrasound was detected while WT 3 was shut down. This can explain the points of low rotational speed in Figure 7a. The two horizontal lines at 12.5 rpm and 12 rpm are the result of a difference in maximum rotational speed during day and night time.

In Figure 7b the relation of infrasonic peak with active power and wind speed of WT 3 is shown. It indicates, that most prominent peaks and highest SPL occur already before rated power is reached at wind speeds above 7 m/s and not necessarily with the highest power output of the WTs as already described in [9]. Furthermore, this is in the range of WT operation in which the maximum rotational speed has already been reached, but the rated wind speed and rated power have not yet been reached. Further investigations into the occurrence of infrasound as a function of rotational speed and active power will be part of future research.

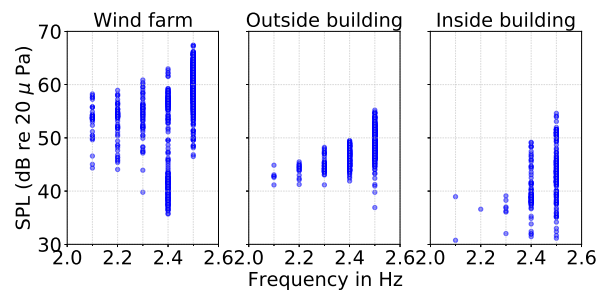


Figure 6: Sound pressure level of 4th blade passing frequency harmonic in relation to frequency in Hz.

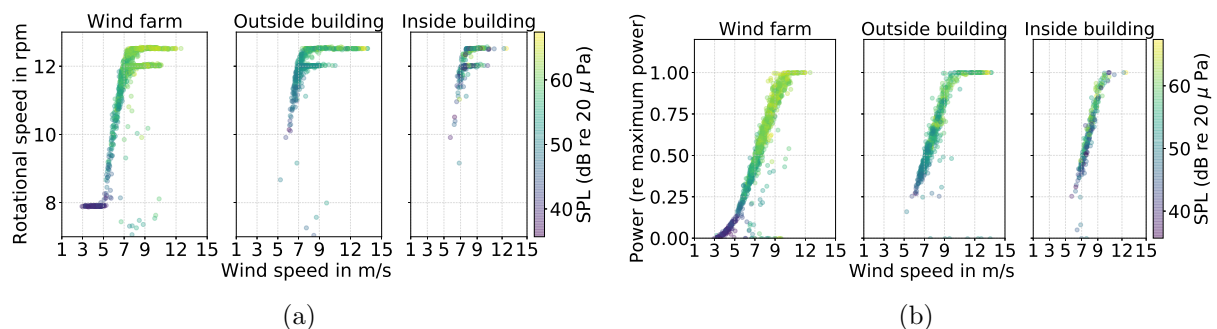


Figure 7: Sound pressure level of 4th blade passing frequency harmonic in relation to rotational speed in rpm (a) and normalized power (b) over wind speed in m/s in hub height of wind turbine 3 during infrasound occurrences.

To identify the impact of wind direction on detected infrasound induced by the WTs, the data are plotted over wind direction of WT 3. Polarplots in Figure 8a-d show the data divided into the measurements periods at R1 to R4. Since the wind direction was not evenly distributed over the four measurement periods, the wind direction of each measurement period must also be considered for comparison. For example, the prevailing wind direction during the measurement period of R1 was south and northwest, indicated by Figure 9a. Accordingly, the wind direction for infrasound occurrences vary within the different measurement periods.

However, on the basis of all the graphs, it can be determined that the SPL of the infrasonic peaks at the WF location is constant at approximately 50 dB to 65 dB for all wind directions. An exception is the period from 2020-11-12 to 2020-11-22 (R2), where infrasound peaks with SPL between 35 dB and 48 dB were detected, but equally constant related to wind direction. The same applies to the values at the residential buildings, with values between 40 dB and 50 dB outside and values varying around 40 dB inside the building. From this it can be concluded that the SPL of the infrasound produced by the WTs is largely independent of the wind direction.

One advantage of this approach is that the detected infrasonic tones can be clearly attributed to the WT operation due to the unique frequency signature, thus preventing the erroneous detection of background noise. Especially in buildings, where the measured spectrum is influenced by noise of everyday life and structural resonances, this could lead to incorrect detection of WT sounds.

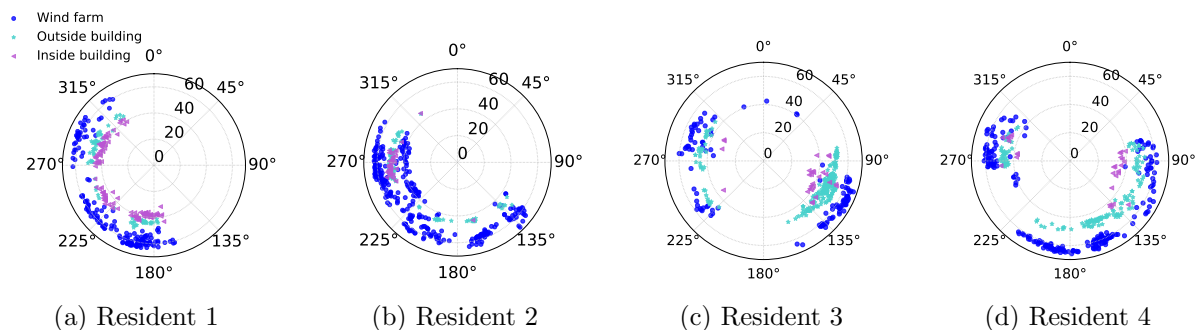


Figure 8: Sound pressure level of 4th blade passing frequency harmonic (in dB re $20 \mu Pa$) for all measuring locations in relation to hub height wind direction of wind turbine 3. Values divided into the four time periods corresponding to the measurement periods at the four residential buildings.

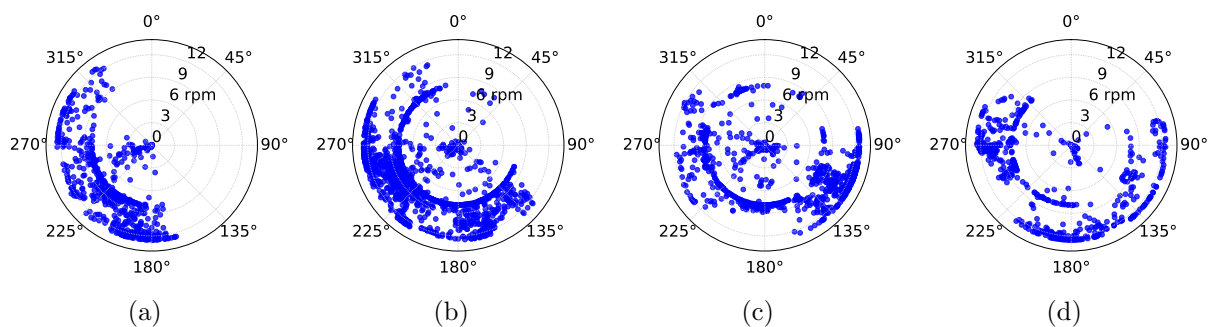


Figure 9: Rotational speed in rpm on the radial axis over wind direction at hub height of wind turbine 3 for the time periods corresponding to the measurement periods at the four residential buildings.

4. Conclusions

In this work the procedure of acoustic measurements in the vicinity of a WF in southern Germany was described. Furthermore acoustic data of three simultaneous measurements at the WF, outside and inside residential buildings were evaluated. To obtain an overview of the frequency components of the sound emissions and immissions, power spectral density diagrams were presented for one exemplary day. The shutdown period of the WTs is clearly recognisable in all measurements by a reduced intensity in the considered frequency range (1-200 Hz). The comparison enables the identification of frequency components that can be assigned to the WT

operation. Narrowband spectra were calculated to determine WT specific noise characteristics more easily for rated and below rated WT operating conditions. Frequency components below 10 Hz can be assigned to the BPF and higher harmonics. Whereas the BPF is more pronounced at all measuring locations during rated WT operation and rarely measured indoors during below rated operation. Tones at 28.9 Hz (rated) and 18.3 Hz (below rated) with two higher harmonics can be attributed to the WT generator. The calculation of 1/3 octave spectra of two exemplary data sets enabled the comparison with the human hearing threshold. Even for a maximum rotational speed of the WTs, the sound pressure level in the infrasound range is far below the audible range of humans.

An analysis of infrasound occurrences showed that the characteristic tones at the BPF were measured at all measuring locations. At residential buildings infrasound is mainly detected for rated condition with maximum rotational speeds between 12 rpm and 12.5 rpm. At all locations highest level of infrasonic tones occur before rated power is reached. Furthermore the SPL of the infrasound peak at all measurement locations seems independent of wind direction.

Although the infrasonic sound components are in the inaudible range, tones of the BPF can be easily attributed to WT operation and could thus provide a tool to detect frequency components in the higher frequency range whose detection is hampered by background noise or structural resonances and which might be amplitude modulated with the BPF, for example. In further studies, the relationship between infrasound occurrence and meteorological conditions needs to be investigated. Additionally the question should be clarified, whether the occurrence of infrasound can indicate simultaneously occurring peculiarities in the audible range of the spectrum, that lead to annoyance in the vicinity of a WF and allow a derivation for noise-reduced WT operation and active control concepts.

4.1. Acknowledgments

We thank the local authorities of the municipality Kuchen for their support, as well as the Stadtwerke Schwäbisch Hall and the KWA Contracting AG for providing operating data. Furthermore we thank Philipp Berlinger for supporting the acoustic measurements. We acknowledge the support of the local residents, who enabled the installation of instruments on their property and within their houses. This study is supported by the Federal Ministry for Economic Affairs and Climate Action based on a resolution of the German Bundestag (grants 03EE2023B).

References

- [1] Tonin R 2012 *Acoustics Australia* **40** 20–27 ISSN 08146039
- [2] Jakobsen J 2005 *Journal of Low Frequency Noise Vibration and Active Control* **24** 145–155 ISSN 20484046 URL <https://doi.org/10.1260/026309205775374451>
- [3] Oerlemans S 2011 *NLR-TP-2011-066* 1–57
- [4] Van Treuren K W 2018 URL <https://zenodo.org/record/1345526>
- [5] Doolan C 2013 *Wind Engineering* **37** 97–104 ISSN 0309524X URL <https://doi.org/10.1260/0309-524X.37.1.97>
- [6] Van Den Berg G P 2005 *Journal of Low Frequency Noise Vibration and Active Control* **24** 1–24 URL <https://doi.org/10.1260/0263092054037702>
- [7] Szulc O 2021 *Archives of Mechanics* **73** 391–417 URL <http://doi.org/10.24423/aom.3756>
- [8] Hansen C H, Doolan C and Hansen K L 2017
- [9] Hansen K, Zajamšek B and Hansen C 2014 *In Proceedings of Internoise, Melbourne, Australia, 16–19 November 2014* 1–11

- [10] Hansen C and Hansen K 2020 *Acoustics* **2** 171–206 URL <https://doi.org/10.3390/acoustics2010013>
- [11] Siponen D 2011 *Technical Research Centre of Finland (VTT), VTT-R-00951-11* 1–26
- [12] Møller H and Pedersen C S 2011 *The Journal of the Acoustical Society of America* **129** 3727–3744 ISSN 0001-4966 URL <https://doi.org/10.1121/1.3543957>
- [13] Oerlemans S 2013 513 URL <http://usir.salford.ac.uk/33475/>
- [14] Doolan C 2011 *Australian Acoustical Society Conference 2011, Acoustics 2011: Breaking New Ground* **40** 494–500 ISSN 2348-4918 URL <http://www.windguard.com/>
- [15] OpenStreetMap 2022-04-07 URL <https://www.openstreetmap.org>
- [16] Blumendeller E, Kimmig I, Huber G, Rettler P and Cheng P W 2020 *Acoustics* 343–365 URL <https://doi.org/10.3390/acoustics2020020>
- [17] Gaßner L, Blumendeller E, Müller F J, Wigger M, Rettenmeier A, Cheng P W, Hübner G, Ritter J and Pohl J 2022 *Renewable Energy* **188** 1072–1093 URL <https://doi.org/10.1016/j.renene.2022.02.081>
- [18] Hunter J D 2007 *Computing in Science & Engineering* **9** 90–95 URL <https://doi.org/10.1109/MCSE.2007.55>
- [19] Virtanen P, Gommers R, Oliphant T E, Haberland M, Reddy T, Cournapeau D, Burovski E, Peterson P, Weckesser W, Bright J and et al 2020 *Nature Methods* **17** 261–272 URL <https://rdcu.be/b08Wh>
- [20] Zajamsek B, Hansen K, Doolan C and Hansen C 2016 *Journal of Sound and Vibration* **370** 176–190 ISSN 0022-460X URL <https://doi.org/10.1016/j.jsv.2016.02.001>
- [21] IEC 61400:2012-11 November 2012 *Wind Turbines—Part 11: Acoustic Noise Measurement Techniques* (International Electrotechnical Committee)
- [22] Cooper J, Evans T and Petersen D 2015 *International Journal of Aeroacoustics* **14** 903–908 ISSN 1475-472X URL <https://doi.org/10.1260/1475-472X.14.5-6.903>
- [23] Hansen K, Hansen C and Zajamsek B 2015 *Building Acoustics Journal* **94** 764–772 ISSN 1351-010X URL <https://doi.org/10.1016/j.buildenv.2015.06.017>
- [24] Hubbard H H 1982 *Noise Control Engineering Journal* **19** 49–55 ISSN 07362501
- [25] Møller H and Pedersen C S 2004 *Noise and Health* **6** 37–57 ISSN 14631741
- [26] DIN 45680:1997-03 March 1997 *Measurement and assessment of low-frequency noise immissions in the neighbourhood* (Berlin: Beuth Verlag)